Origin of the diverse behavior of oxygen vacancies in ABO_{3} perovskites: A symmetry based analysis

Wan-Jian Yin, Su-Huai Wei, Mowafak M. Al-Jassim, and Yanfa Yan

Phys. Rev. B **85**, 201201 — Published 14 May 2012

DOI: 10.1103/PhysRevB.85.201201

Origin for the diverse behavior of oxygen vacancies in ABO_3 perovskites: A symmetry based analysis

Wan-Jian Yin[1,*], Su-Huai Wei[2], Mowafak M. Al-Jassim[2] and Yanfa Yan[1]
[1]*Department of Physics & Astronomy, University of Toledo, 2801 Bancroft Street, Toledo, OH 43606*
[2]*National Renewable Energy Laboratory, Golden, CO 80401*

ABSTRACT

Using band symmetry analysis and density functional theory calculations, we reveal the origin of why oxygen vacancy (V_O) energy levels are shallow in some ABO_3 perovskites, such as $SrTiO_3$, but are deep in some others, such as $LaAlO_3$. We show that this diverse behavior can be explained by the symmetry of the perovskite structure and the location (A or B site) of the metal atoms with low *d* orbital energies, such as Ti and La atoms. When the conduction band minimum (CBM) is an anti-bonding Γ_{12} state, which is usually associated with the metal atom with low *d* orbital energies at the A site (e.g., $LaAlO_3$), then the V_O energy levels are deep inside the gap. Otherwise, if the CBM is the non-bonding $\Gamma_{25'}$ state, which is usually associated with metal atoms with low *d* orbital energies at the B site (e.g., $SrTiO_3$), then the V_O energy levels are shallow and often above the CBM. The V_o energy level is also deep for some uncommon ABO_3 perovskite materials that possess a low *s* orbital, or large-size cations, and an anti-bonding Γ_1 state CBM, such as $ZnTiO_3$. Our results, therefore, provide guidelines for designing ABO_3 perovskite materials with desired functional behaviors.

PACS number: 71.15.Mb; 71.20.Nr; 71.55.-I

ABO_3 perovskites are group of materials that possess many interesting physical properties and functional behaviors, such as ferroelectricity, superconductivity, and photoelectrochemical sensitivity [1]. It has been observed that the properties and functional behaviors of the perovskites are heavily influenced by the presence of oxygen vacancies (V_O) in these materials. For example, the insulator-to-metal transition, observed in $SrTiO_{3-x}$, can occur when a certain amount V_O is introduced [2]. The free carriers that are responsible for the blue-light emission of Ar^+-irradiated $SrTiO_3$ (STO) at room temperature are generated by V_O [3]. The recently discovered two-dimensional conducting electron gas (2DEG) at the interface of STO and $LaAlO_3$ (LAO) [4, 5] can also be linked to the formation of V_O in STO and LAO; conductivity was observed when a significant concentration of V_O was introduced in the STO/LAO system [6-8]. Interestingly, however, advanced conducting-tip atomic force microscope (CT-AFM) measurements show that the spatial carrier density extends from the interface to the STO side but not to the LAO side [9]; this seems to indicate that the V_O could be shallow donors in STO, but they produce deep levels in LAO. This conjecture is also consistent with recent experimental observation that V_O could result in 2DEG at the surface of STO even without the existence of LAO [10, 11]. This puzzling behavior of V_O in perovskites, i.e., V_O levels are shallow in some perovskites such as STO but deep in some others such as LAO, is fascinating. However, so far, the origin for this puzzling behavior and its relationship to the band structure of the perovskites are still not known. Understanding these issues will shed light on understanding the unique electronic and optoelectronic properties of ABO_3 perovskites and help in designing perovskites with new and desirable properties and functional behaviors.

In this Letter, we elucidate the origin of the various behavior of V_O in ABO_3 perovskites using band symmetry analysis and density functional theory (DFT) calculations. We show that

the interesting behavior of V_O in ABO_3 perovskites originates from the symmetry of the perovskite structure and the location (A or B site) of the transition metal (TM) atoms (e.g., Ti or La in the crystal). The conduction band minimum (CBM) of common perovskites can be either the anti-bonding Γ_{12} state or the non-bonding $\Gamma_{25'}$ state as derived from TM *d* orbitals. V_o levels could be shallow when the CBM is derived from the non-bonding $\Gamma_{25'}$ state, as in the case of STO. However, the V_o levels are deep if the CBM is derived from the anti-bonding Γ_{12} state, as in the case of LAO. We also find that the V_o levels are deep for some uncommon perovskites, such as $ZnTiO_3$, when their CBM is the anti-bonding Γ_1 state.

The structural and electronic properties of perovskite crystals are calculated by using a hybrid density functional (HSE06) (with exact exchange part $\alpha = 0.25$) [12] as implemented in VASP code [13] using standard frozen-core projector augmented-wave (PAW) method [14]. The cut-off energy for basis functions is 400 eV. The primitive cell of perovskite structure ($Pm\bar{3}m$) is a five-atom cube [Fig. 2(c) and (f)], in which a Γ-centered (7×7×7) *k*-ponit mesh is used. For the study of the isolated V_o point defect, the (3×3×3) host supercell containing 134 atoms (with the removal of one O atom) is used. Only the Γ point is used for the Brillouin zone integration. The (3×3×3) supercell is found to be large enough in the defect calculation. The calculations with different methods including different α in HSE06 and local density approximation (LDA) were also applied and we found that our conclusion did not change [15].

In the cubic perovskite structure, O atoms are at the face centers with a local D_{4h} point group symmetry. The TM atoms at both the A and B sites have the local point group symmetry O_h, allowing the *d* orbitals to split into triply degenerated t_{2g} states (d_{xy}, d_{yz}, d_{zx}) and doubly degenerated e_g states (d_{z2}, d_{x2-y2}). However, because of the different local environment (12 nearest O neighbors at the A sites and 6 nearest O neighbors at the B sites), the Coulomb repulsion

induced crystal field splitting of the *d* states, E(t_{2g}) – E(e_g), is significantly different for the TM atoms at the A sites compared to the B sites; t_{2g} states are higher than e_g states if the TM atoms are at the A site, but it is exactly the opposite, e_g states are higher than t_{2g} states, if the TM atoms are at the B site (Fig. 1). Because of the O_h symmetry, the metal *d* states do not couple with O *p* states with t_{1g} and t_{2u} symmetry at the Brillouin zone center, but the e_g states can couple with O *s* state [16-18]. The coupling of the O *s* states and cation *s* states can also form a_1 states. As we will show later, the electronic structures and behavior of V_O vary greatly depending on which state derives the CBM of the perovskites. For common perovskites, there are two scenarios: the CBM is derived from either the anti-bonding Γ_{12} states or the non-bonding $\Gamma_{25'}$ states. Our findings show that V_o levels could be shallow *only* when the CBM has the non-bonding $\Gamma_{25'}$ characteristic, which is the case for STO. We also find that the V_o levels are deep for some uncommon ABO_3 perovskite materials, such as $ZnTiO_3$, where their CBM has the anti-bonding Γ_1 characteristic.

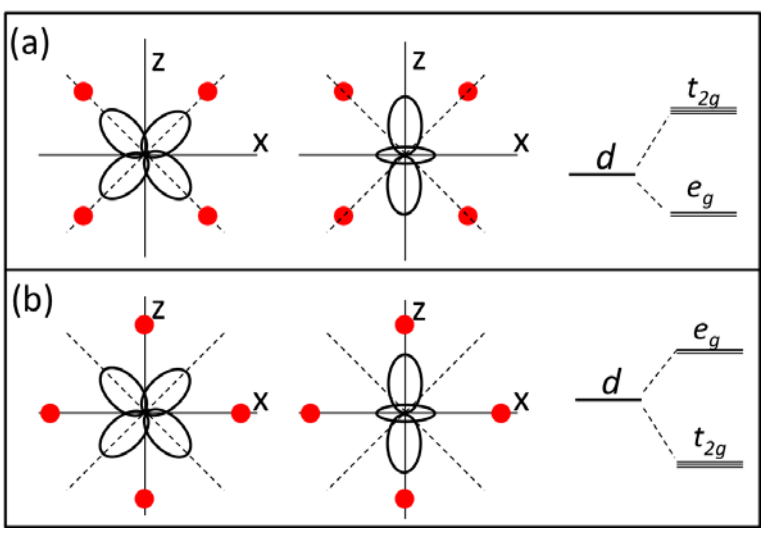

Figure 1: (Color online) The schematic picture of the t_{2g} and e_g splitting of transition metal atoms at (a) A and (b) B sites of perovskite ABO_3. The orbitals of d_{xz} (left panel) and d_{z^2} (middle panel)

are chosen as representatives of t_{2g} and e_g states, respectively. The red (solid) dots are the positions of oxygen atoms.

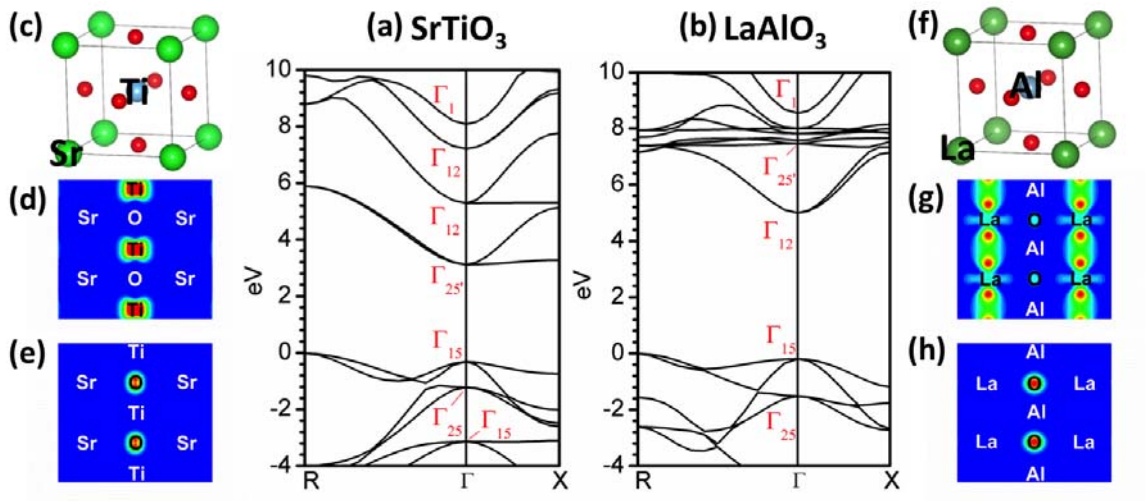

Figure 2: (Color online) (a) and (b) are the HSE06 calculated band structures of $SrTiO_3$ and $LaAlO_3$, respectively, with zero energy at the VBM. The primitive cells of (c) $SrTiO_3$ and (f) $LaAlO_3$ and the partial charge densities of the CBM of (d) $SrTiO_3$ and (g) $LaAlO_3$ are depicted; (e) and (h) show the partial charge densities of the VBM at the Γ point of $SrTiO_3$ and $LaAlO_3$, respectively, plotted in the (110) plane.

Figure 2 shows the crystal structure of STO and LAO and the calculated band structures using the HSE06 functional. For a typical ABO_3 perovskite [19], such as STO, the valence bands at the Brillouin zone center have bonding O *s* derived Γ_1 states and TM *s, d* derived Γ_{12} states, respectively, (not shown in Figure 2), in addition to O *p* derived Γ_{15} and Γ_{25} states at the top of valence bands. The conduction bands have the non-bonding $\Gamma_{25'}$ (TM t_{2g}), anti-bonding Γ_{12} (TM e_g + *O s*), and anti-bonding Γ_1 (TM *s* + O *s*) states [20]. As the coupling between O *s* and cation *s* is usually stronger than that between O *s* and TM e_g states, the Γ_{1c} state is usually higher in energy than the Γ_{12c} states, whereas the Γ_{1v} state is usually lower in energy than the Γ_{12v} states

(see Fig. 2a and 2b). Therefore, the energy sequence in the valence band is $\Gamma_{15} > \Gamma_{25} > \Gamma_{15} > \Gamma_{12} > \Gamma_1$, with the valence band minimum (VBM) in an anti-bonding oxygen *p* state. In the conduction band, the CBM usually has a TM *d* characteristic. However, there could be exceptions, which we will discuss later. The interesting issue is that the state of the CBM (non-bonding $\Gamma_{25'}$ state or the anti-bonding Γ_{12} state) depends on the position of the TM with low energy *d* orbitals. As discussed earlier, for systems, such as STO (Fig. 2c), with transition metal atoms (Ti) located at the B site, the charge density lobes of the e_g states point along the bond direction (Ti-O), while the charge density lobes of the t_{2g} states do not (Fig. 1b). The Coulomb repulsion between the electronic orbitals pushes the e_g states higher in energy than the t_{2g} states. Consequently, the CBM is derived from the non-bonding $\Gamma_{25'}$ states. On the other hand, if the TM atom with low *d* orbital energy is at the A site, such as LAO (Fig. 2f), the situation is reversed; the wavefunctions of the t_{2g} states point along the bond direction (La-O), while the wavefunctions of the e_g states do not (Fig. 1a). Thus, t_{2g} states are now at a higher energy level than the e_g states, such that the CBM is derived from the anti-bonding Γ_{12} states. The coupling with the O s states would shift the e_g states up slightly, but the effect of the coupling is usually not as strong as crystal field splitting and does not reverse the order.

In the following section, we will show that the nature of V_O levels is determined by the character of the CBM, that is, whether the CBM has the Γ_1, Γ_{12}, or $\Gamma_{25'}$ symmetry.

(i) The CBM is the non-bonding $\Gamma_{25'}$ state. In this case, as discussed above, the TM atoms are at the B site, and STO will serve as a typical example. The band structure of STO definitely shows the CBM with the $\Gamma_{25'}$ symmetry [Fig. 2(a)]. There are two Γ_{12} states above $\Gamma_{25'}$. The lower state is derived mainly from Ti 3*d*, and the higher state is derived mainly from Sr 4*d*. The partial charge densities [Fig. 2(d) and Fig. 2(e)] show that the VBM is nearly comprised of a pure

O *p* characteristic and the CBM has a pure Ti *d* characteristic: which is consistent with the symmetry analysis described above. As the CBM of STO ($\Gamma_{25'}$) is derived from the non-bonding Ti t_{2g} states, the removal of one O atom, i.e., the formation of a V_O, only lowers the energy of the anti-bonding Γ_{12} state to nearly the Ti e_g states [21]. The V_o, though, does not influence the $\Gamma_{25'}$ CBM state (close to Ti t_{2g} states) much. This process creates the V_O energy levels in ABO_3 perovskite crystals. Because the Ti e_g states are higher in energy than the Ti t_{2g} states, the V_O levels are above the CBM [Fig. 3(b)(c) and see Ref. [15] for how the level of V_O is determined]. Consequently, a V_O will spontaneously donate its two electrons to the CBM, and therefore, the V_O is *automatically* ionized and it is always at the V_O^{2+} state. In this case, it is not meaningful to calculate the transition energies because the neutral and 1+ charged V_O states are unstable. We find that for the V_O^{2+} state, the resonant V_O level with mainly the Ti e_g characteristic is 1.23 eV higher than the CBM [Fig. 3 (b)]. This high defect level is partially due to the outward relaxation of the cations for the V_o^{2+} charged state. The charge distribution, around the V_o site, of this state is shown in Fig. 3(a). The location of the V_O is indicated by the open, red square. Due to its resonant nature, though, this state is not very localized.

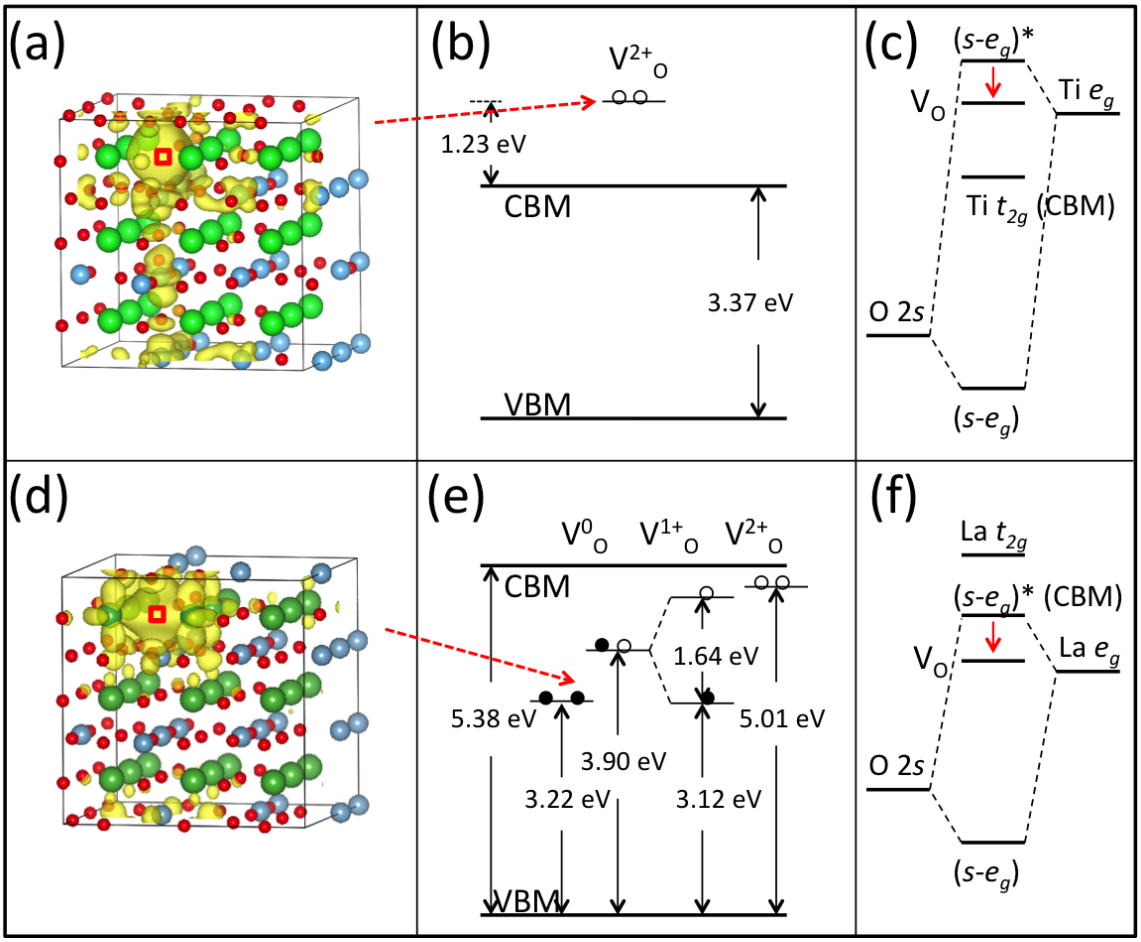

Figure 3: (Color online) The partial charge density of the single electron defect level of V_O^{2+} at the Γ point in (a) STO and V_O^0 in (d) LAO. The red (open) squares indicate the location of V_O. (b) and (e) show the energy positions of V_O levels in STO and LAO, respectively. (c) and (f) show the schematic mechanisms of how the V_O's are formed in STO and LAO, respectively, and why the V_O levels are shallow or deep.

(ii) The CBM is the anti-bonding Γ_{12} state. In this case, as discussed above, the TM atoms are at the A site, and LAO will serve as a typical example. The band structure of LAO is shown in Fig. 2(b). The VBM has a nearly pure O *p* characteristic, precisely like STO. However, unlike the

case of STO, the CBM of LAO is the Γ_{12} state, which is derived from the anti-bonding states of O *s* and La 5*d* e_g states. The removal of an O atom (formation of an V_O) will lower the position of the Γ_{12} to nearly that of the La e_g states and form the V_O levels deep inside the gap, as indicated in Fig. 3(f). Our HSE06 calculation confirmed that the single electron level of V_O^0 is 2.16 eV below the CBM for LAO. The calculated charge distribution of this defect level shows that the wavefunction is more localized around the V_O site [Fig. 3(d)] as compared to the case of STO [Fig. 3(a)]. This result is consistent with the fact that the V_o state is deep inside the gap. The single electron energy levels of this state increase in energy as the V_O is ionized to a 1+ and 2+ charged state [Figs. 3(e)] due to the large atomic displacement around the defect site when V_O is charged. Like most oxides, V_O in LAO is a negative U system.

(iii) The CBM is the Γ_1 state. This situation is very rare because Γ_1 is the anti-bonding state of cation *s* and O *s*, and the coupling is usually large. To let the Γ_1 state drop below the Γ_{12} and $\Gamma_{25'}$ states, one could either increase the cation size to reduce the interaction strength or choose cations with low unoccupied *s* states and high unoccupied *d* orbital energy. $ZnTiO_3$ is a good example since Zn has a much lower *s* orbital energy than alkaline earth metal elements and its unoccupied 4*d* orbitals are much higher in energy. HSE06 calculated the direct band gap of $ZnTiO_3$, at the Γ point, to be 1.31 eV, with the Zn *s* derived Γ_1 state 2.68 eV lower than the Ti t_{2g} derived $\Gamma_{25'}$ state. The artificial material $LuInO_3$ is another example of a Γ_1 CBM state, where both Lu and In have large atomic radii. As a result, the Lu *s* derived anti-bonding states (Γ_1) have weak coupling strength and drop below its t_{2g} and e_g states. The calculated single electron levels of V_O^0 of $ZnTiO_3$ and $LuInO_3$ are 0.22 eV and 0.37 eV, respectively, below their CBM's level. This result is consistent with the picture that the V_O should be deep when the CBM is not the $\Gamma_{25'}$ state.

Based on the analysis of the relationship between the band structures and V_O properties of the ABO_3 perovskites discussed above, we can now provide general rules to estimate the V_O properties of perovskite oxides. For example, the V_O's are usually shallow for most IIA-VIB-O_3 and IA-VB-O_3 perovskites ($BaTiO_3$, $KTaO_3$, etc. [22, 23]) since their bulk CBMs are $\Gamma_{25'}$ states like $SrTiO_3$. The V_O levels are deep in $LaAlO_3$, $YAlO_3$ and $LuAlO_3$ [24] since the TM atoms, with low lying *d* orbital (i.e., Y and Lu), are on the A site, and the CBM is the anti-bonding Γ_{12} state: as is the case for LAO. Therefore, it is likely that $BaTiO_3$, $KTaO_3$ will be conductive if V_O's are introduced [22, 23]. On the other hand, $LaAlO_3$, $YAlO_3$ and $LuAlO_3$ [24] would be intrinsically insulators.

In conclusion, using band structure symmetry analysis and density functional theory calculation, we have revealed the origin of the unusual behavior of oxygen vacancies in common ABO_3 perovskites. We found that when transition metal atoms are at the A site, the CBM is usually the anti-bonding state of the transition metal *d* and the O *s* (a Γ_{12} state), and the oxygen vacancy levels will be deep. However, when transition metal atoms are on the B site, the CBM is usually the non-bonding transition metal t_{2g} states (a $\Gamma_{25'}$ state), and the oxygen vacancy levels will be shallow. We also found that the oxygen vacancy levels are deep in perovskites with low cation *s* orbital or large cation sizes, and whose CBM is the anti-bonding *s* state (a Γ_1 state). Our results, therefore, explain why $SrTiO_3$ and $LaAlO_3$ behave so differently and provide guidelines for designing functional perovskites with desired conductivity.

Work at NREL was supported by the U.S. Department of Energy under Contract No. DE-AC36-08GO28308. The computation was partially supported by the Ohio Supercomputer Center. Y.Y. Acknowledges the support from the Ohio Research Scholar Program (ORSP).

Corresponding author: wanjian.yin@utoledo.edu

References

[1] T. Wolfram and S. Ellialtioglu, *Electronic and Optical Properties of d-Band Perovskites* (Cambridge University Press, Cambridge, England, 2006).

[2] Z. Liu, D. P. Leusink, X. Wang, W. M. Lu, K. Gopinadhan, A. Annadi, Y. L. Zhao, X. H. Huang, S. W. Zeng, Z. Huang, A. Srivastava, S. Dhar, T. Venkatesan, and Ariando, *Phys. Rev. Lett.* **107**, 146802 (2011).

[3] D. Kan, T. Terashima, R. Kanda, A. Masuno, K. Tanaka, S. Chu, H. Kan, A. Ishizumi, Y. Kanemitsu, Y. Shimakawa, and M. Takano, *Nature Mater.* **4**, 816 (2005).

[4] D. A. Muller, N. Nakagawa, A. Ohtomo, J. L. Grazul, and H. Y. Hwang, *Nature (London),* **430**, 657 (2004).

[5] A. Ohtomo and H. Hwang, *Nature* **427**, 423 (2004).

[6] W. Siemons, G. Koster, H. Yamamoto, W. A. Harrison, G. Lucovsky, T. H. Geballe, D. H. A. Blank, and M. R. Beasley, *Phy. Rev. Lett.* **98**, 196802 (2007).

[7] G. Herranz, M. Basletic, M. Bibes, C. Carretero, E. Tafra, E. Jacquet, K. Bouzehouane, C. Deranlot, A. Hamzic, J.-M. Broto, A. Barthelemy, and A. Fert, *Phy. Rev. Lett.* **98**, 216803 (2007).

[8] A. Kalabukhov, R. Gunnarsson, J. Borjesson, E. Olsson, T. Claeson, and D. Winkler, *Phys. Rev. B* **75**, 121404(R) (2007).

[9] M. Basletic, J.-L. Maurice, C. Carretero, G. Herranz, O. Copie, M. Bibes, E. Jacquet, K. Bouzehouane, S. Fusil, and A. Barthelemy, *Nature Mater.* **7**, 621 (2008).

[10] A. F. Santander-Syro, O. Copie, T. Kondo, F. Fortuna, S. Pailhes, R. Weht, X. G. Qiu, F. Bertran, A. Nicolaou, A. Taleb-Ibrahimi, P. Le Fevre, G. Herranz, M. Bibes, N. Reyren, Y. Apertet, P. Lecoeur, A. Barthelemy, and M. J. Rozenberg, *Nature (London)* **469**, 189 (2011).

[11] W. Meevasana, P. D. C. King, R. H. He, S-K. Mo, M. Hashimoto, A. Tamai, P. Songsiriritthihul, F. Baumberger, and Z-X. Shen, *Nature Mater.* **10**, 114 (2011).

[12] J. Paier, M. Marsman, K. Hummer, G. Kresse, I.C. Gerber, and J.G. Ángyán, *J. Chem. Phys.* **124**, 154709 (2006).

[13] G. Kresse and J. Furthmuller, *Phys. Rev. B* **54**, 11169 (1996); *Comput. Mater. Sci.* **6**, 15 (1996).

[14] P.E. Blochl, **50**, 17953 (1994); G. Kresse and D. Joubert, *Phys. Rev. B* **59**, 1758 (1999).

[15] See Supplemental Material at [*URL will be inserted by publisher*] for the supercell size convergence, the methods we used and also how the V_O level is determined in $SrTiO_3$.

[16] J. F. Cornwel, *Group Theory and Electronic Energy Bands in Solids* (North-Holland Publishing Company, London, 1969).

[17] M. S. Dresselhaus, G. Dresselhaus, and A. Jorio, *Group Theory : Application to the Physics of Condensed Matter* (Springer-Verlag, Berlin, 2008).

[18] R. F. Berger, C. J. Fennie, and J. B. Neaton, *Phys. Rev. Lett.* **107**, 146804 (2011).

[19] L. F. Mattheiss, *Phys. Rev. B* **6**, 4718 (1972)

[20] The cations in the typical perovskite discussed in this letter have d^0 or d^{10} configuration. The cations with interesting p orbital, such as Pb, contribute Γ_{15} (t_{1u}) instead of Γ_1 (a_1) in CB. We consider only Γ_1 here in our general band structure analysis, however, the physics picture is the same if the CBM has the Γ_{15} symmetry.

[21] W.-J. Yin, S.-H. Wei, M. Al-Jassim, and Y. Yan, *Appl. Phys. Lett.* **99**, 142109 (2011).

[22] M. Choi, F. Oba, I. Tanaka, *Phys. Rev. Lett.* **103**, 185502 (2009).

[23] M. Choi, F. Oba, I. Tanaka, *Phys. Rev. B* **83**, 214107 (2011).

[24] D. J. Singh, *Phys. Rev. B* **76**, 214115 (2007).